Control strategy of Grid-Connected PV Inverters in Microgrid with Nonlinear Operating Conditions

1nd A. Naderipour and 2nd * Z. Abdul-Malek
Institute of High Voltage & High Current, School of Electrical Engineering, Faculty of Engineering, Universiti Teknologi Malaysia,
81310 Johor Bahru, Malaysia
namirreza@utm.my
zulkurnain@utm.my*

3nd E. Abohamzeh
Department of Energy,Material and Energy Research Center (MERC),
Karaj, Iran.
elhamaboohamzeh@gmail.com

5th M. R. Miveh
Department of Electrical Engineering, Tafresh University
Tafresh, 39518-79611, Iran
miveh@tafresh.ac.ir

4rd Vigna K. Ramachandaramurthy
Institute of Power Engineering, Dept. of Electrical Power Engineering, Universiti Tenaga Nasional, Jalan IKRAM-UNITEN
43000 Kajang, Selangor, Malaysia
vigna@uniten.edu.my

***Abstract*—This paper proposes a current control strategy for a Photovoltaic (PV) system in three-phase three-wire grid-connected microgrids under unbalanced and nonlinear load conditions. The proposed control strategy comprise of a multi-loop control technique to provide balanced output current, multi-resonant harmonic compensator to reduce the Total Harmonic Distortion (THD) and a droop-based control scheme to achieve accurate power sharing. Additionally, the current THDs were reduced from above 17.51% to lower than 3% with the proposed control strategy under nonlinear load conditions. The effectiveness of the proposed control strategy was proven via simulation using MATLAB/Simulink.**

Keywords—Current control, Microgrid, Photovoltaic, Harmonics, Grid-connected Inverter

I. INTRODUCTION

Traditional large power plants in the form of hydro, coal or gas are known to provide reliable power supply. However, the concern for the environment and economy have led to the gradual deployment of small-scale power sources in the form of renewable energy into the electrical grid. Microgrid (MG) typically consists of Distributed Generations (DGs), load, smart communication and protection devises and Energy Storage Systems (ESS). Microgrid requires a flexible control system that is appropriate for both grid-connected and islanded operations. The addition of significant levels of renewable generators, such as Photovoltaics (PVs), may increase the complexity of the electrical grid due to the uncertain nature of the energy sources. For example, the intermittency of these renewable energy plants may add complexity to the grid operation when combined with load variability [1]. Thus, studies are required to determine the operating conditions when new DGs are connected.

Typically, renewable energy type DGs such as solar PV and wind turbines are connected to grid via converters [2]–[4]. These converter would have a cascade of two or more control loops. One of these loops would be a fast internal loop, and it is in charge of the injected current. The second loop would be an external loop that controls the DC link voltage. The internal loop shall also handle harmonic compensations. In [5], a mathematical model was developed for a passive Hamiltonian system. It was integrated with a grid-connected inverter, which was equipped with an LC filter. This control system is capable of achieving the static and dynamic features of a grid-connected inverter, including its ability to mitigate harmonics. Hence, a newly developed topology of a grid-connected inverter was applied to the Microgrid. It has numerous functions, which include simultaneously compensating the harmonics, unbalance, and reactive currents of the MG. This system was also fitted with a parallel controller, which depends on the weighted current feedback, and hysteresis current loop.

Dong and his co-workers [6] proposed a state feedback quasi-static Synchronous Reference Frame Phase Locked Loop (SRF-PLL) model for a converter control system. This model can pinpoint, and assess the latent frequency self-synchronization mechanism in the system. The effect of self-synchronization is due to the interactions between the converter, the grid impedance, and power flow directions. Authors in [7] studied the application of a Constant Power Load (CPL) for shunt active filtering in a system that receives constant active power from the source. CPL control applies vector control method, and it is a part of the reference signal generation techniques for shunt compensators. These techniques comply with the Instantaneous Reactive Power (IRP) p-q and the Current's Physical Components (CPC) theory in synchronous rotating reference frame. Chunkag et al. [8] reported a current control system in a *dq* frame for an AC to DC converter. This system converts an orthogonal current from the actual input current, and the $e^{-sT/4}$ delay current from their stationary frame to a rotating frame. Therefore, these steady-state current components will become direct currents as opposed to alternating current values, which gives zero steady-state error. Power calculation can also be easily determined for this system.

In [9], two methods of unit template-based AC current control schemes were proposed. The first method applied phase information from PLL, while the second one used voltage peak estimates. The SRF-PLL has fluctuating behaviors due to the PI gains being affected by the harmonic rejection bandwidth, which often causes a slow response. Conversely, a unit template voltage-based hysteresis current controller with faster responses would come attached with high harmonic contents. Therefore, they proposed a Filtered Unit Template (FUT) control strategy to phase out the harmonics. Waleed Al-Saedi and his co-workers [10] were able to develop an ideal power control strategy. This strategy was used with an inverter-based DG unit for an autonomous MG. Nonetheless, this approach decreases the controller gain whenever a disturbance or set-point change occurs. This turns the controller into a 'cautious' one that averts any possible overshoots. It can be 'aggressive' again by modifying the effective loop, which would result in larger controller gains for large set-point errors.

To overcome these challenges, this paper has proposed a current control strategy using a rotating reference frame current controller under unbalanced and nonlinear load conditions in a microgrid. This proposed control scheme has the ability to provide balanced output current under highly unbalanced load conditions with fast dynamic response, and a good steady-state performance. Additionally, it can reduce the current THD of the grid-following power converter under nonlinear load conditions, utilizing a simple control algorithm.

II. RESEARCH METHOD

The control loops which controls the DC-link voltage, can be structured by utilizing the stationary reference frame. This control strategy involves using the *abc* to *αβ* module to transform grid currents into a stationary reference frame. The control variables are sinusoidal, thus, the PI controller would be unfavorable for this strategy. PI controller is unable to eliminate steady-state error, thus other types of the controller would be needed to control the sinusoidal waveforms. Recently, the Proportional-Resonant (PR) controller [11] became more favorable for applications in grid-tied systems. The controller matrix for PR controller in the stationary reference frame is represented by the following equation (1):

$$G_{PR}^{(\alpha\beta)}(s)=\begin{bmatrix} K_p+\dfrac{K_i s}{s^2+\omega^2} & 0 \\ 0 & K_p+\dfrac{K_i}{s^2+\omega^2} \end{bmatrix} \quad (1)$$

where ω is the resonance frequency of the controller, k_p is the proportional gain, and k_i is the integral gain of the controller. The PR controller is capable of attaining higher gains around the resonance frequency. Hence, it is suitable for eliminating the steady-state error that occur between the controlled signal and its reference [12]. The integral gain of the controller (k_i) dictates the frequency band's measurement around the resonance point, whereby a very narrow band indicates a low k_i, while a wider band indicates a high k_i. Applying a PR controller in the natural reference frame (*abc*) is a direct process because it is in the stationary frame. Equation (2) shows how to apply three controllers into the *abc* frame. Nonetheless, this current study took into account the effect of the isolated neutral in the control, which did not require three controllers, as indicated by equation (2).

$$G_{PR}^{(abc)}(s)=\begin{bmatrix} K_p+\dfrac{K_i s}{s^2+\omega_0^2} & 0 & 0 \\ 0 & K_p+\dfrac{K_i s}{s^2+\omega_0^2} & 0 \\ 0 & 0 & K_p+\dfrac{K_i s}{s^2+\omega_0^2} \end{bmatrix} \quad (2)$$

The PR controller enables high gains around the natural resonant frequency of *ω*. This enables the mitigation of low order harmonics.

A. Grid-Connected Performance

The following characteristics were applied to control P^+ and Q^+ in the microgrid that was connected to the main grid:

$$\emptyset^* = \emptyset_0 + \left(k_{pP} + \frac{k_{iP}}{s}\right).\left(P^{+^*} - P^*\right) \quad (3)$$

$$E^* = E_0 + \left(k_{pQ} + \frac{k_{iQ}}{s}\right).\left(Q^{+^*} - Q^*\right) \quad (4)$$

In these equations, P^{+^*} and Q^{+^*} are the reference values of powers, and k_{iQ} is the integral coefficient of reactive power.

Equation (4) acts as a PI controller for voltage with the aim of bringing injection reactive power by the DG to the reference value. P^{+^*} can be determined in a similar manner to the maximum value of power produced by the original source of DG. For example, MPPT can be used to determine P^{+^*} (even in islanded mode) in the case of a solar system. Additionally, Q^{+^*} can be set as zero in order to achieve unity power factor or a positive value to support the reactive power of the network. The P^{+^*} and Q^{+^*} can also be determined by a central controller with the aim of optimizing the economic performance of the microgrid. By incorporating equation 5) into 6) with the assumption of $\emptyset \approx 0$, small-signal dynamic of closed-loop transfer function can be expressed as follows:

$$\hat{P} = 3.\frac{V}{L_{v.s}}\left(E.\cos\emptyset.\hat{\emptyset} + \hat{E}.\sin\emptyset\right) \quad (5)$$

$$\hat{Q} = 3.\frac{V}{L_{v.s}}\left(\hat{E}.\cos\emptyset - \hat{E}.\sin\emptyset.\hat{\emptyset}\right) \quad (6)$$

$$s^6 + As^5 + Bs^4 + Cs^3 + Ds^2 + Es + F = 0 \quad (7)$$

which in this equation:

$$\begin{aligned} A &= 2.\omega_c, \\ B &= \omega_c\left[\omega_c + \frac{3.V}{L_v}\left(E.k_{pP} + k_{pQ}\right)\right], \\ C &= \frac{3.\omega_c.V}{L_v}\left[E\left(k_{iP} + \omega_c + k_{pP}\right) + \omega_c.k_{pQ} + k_{iQ}\right], \\ D &= \frac{3.\omega_c^2.V}{L_v}\left[\left(k_{iP} + \frac{3.V.k_{pQ}.k_{pP}}{L_v}\right) + k_{iQ}\right], \\ E &= \frac{9.\omega_c^2.V^2.E}{L_v^2}\left(k_{pQ}.k_{iP} + k_{iQ}.k_{pP}\right), \\ F &= \frac{9.\omega_c^2.V^2.E.k_{iQ}.k_{iP}}{L_v^2} \end{aligned} \quad (8)$$

Based on equation (7), the parameters of the power controllers can be selected in such a way that the stability of the closed-loop system is maintained. It should be noted that

similar stability analysis can be done to select the maximum value of droop characteristic parameters in islanded mode.

B. Compensation of the Microgrid Current Harmonics

Figure 1 shows the structure and control system of the microgrid in grid-connected mode. Two separate compensation modes; compensation of voltage harmonics, and of current harmonics were considered. In situations where sensitive loads are connected to the PCC, voltage harmonics can be compensated to provide high voltage quality in PCC. In addition, compensation of PCC voltage harmonics may impact power quality distortions in any of the networks (microgrid or core network), where power quality of each side is reduced. In the absence of sensitive loads in PCC, and no significant effect of network disturbances, current harmonics compensation mode was selected to avoid excessive injection of harmonic current by the main network. The current control mode could reduce the thermal stress generated in the grid-connected transformer, which resulted in passing harmonic currents. Additionally, PCC bus voltage distortion which is caused by the flow of harmonic currents, can be avoided. In both cases, compensation can be achieved with proper control of the interface converter of DGs. Microgrids can be connected to the main network through a distribution line with Z_g impedance and a transformer with equivalent Z_t impedance. It was observed that the harmonic orders of PCC voltage (v_{PCCabc}) and network current (i_{gabc}) were extracted by the measurement blocks, v^h_{dq} and i^h_{dq} , as the *h* order harmonic of voltage and current, respectively, and sent to all DGs.

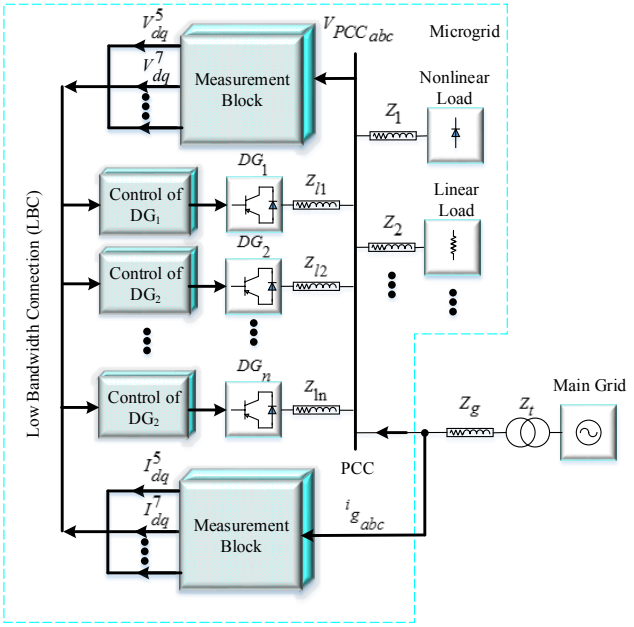

Fig. 1. Structure and control system of the microgrid in grid-connected mode

Compensation was done selectively for the main harmonics of the PCC. Thus, it was necessary that the data related to these harmonics are extracted and sent. Given that PCC could be at a distance from DGs, Low Bandwidth Communication (LBC) was used to send voltage and current harmonics data. The low bandwidth was used for this purpose because the performance of the control system does not depend on the availability of high bandwidth. Thus, the reliability was increased, while decreasing the cost of providing high bandwidth. It was assumed that data transmission through LBC has 1 ms delay.

To ensure that the LBC has enough data transmission, the transmitted data should be entirely DC signals. Thus, harmonic components of PCC and network current were extracted in the reference frame, *dq*.

Park transformation relation, which is shown by the following equation (9), was used for variable transmission from frame *abc* to frame *dq* in which θ is the rotation angle of frame *dq*:

$$x_{dq} = \sqrt{\frac{2}{3}}\begin{bmatrix} \cos\theta & \cos\left(\theta-\frac{2\pi}{3}\right) & \cos\left(\theta+\frac{2\pi}{3}\right) \\ \sin\theta & \sin\left(\theta-\frac{2\pi}{3}\right) & \sin\left(\theta+\frac{2\pi}{3}\right) \end{bmatrix} x_{abc} \qquad (9)$$

The proposed control method of extracting PCC voltage harmonics in measurement blocks are shown in Figure 2. For this purpose, (v_{PCCabc}) was initially transferred to the rotating reference frame at a speed proportional to the harmonics. For example, speeds of -5ω and 7ω (corresponding to θ-5ωt, and θ=7ωt, respectively) were used to extract the fifth and seventh harmonics (v^5_{dq}, v^7_{dq}). ω is the angular frequency of the system that is extracted by PLL. Then, second-order Low-Pass Filter (LPF) with cutoff frequency (ω_{cut}=4π*rad/s)* of 2 Hz, and damping ratio of ζ=0.707 were used to calculate the harmonic voltages of frame *dq*. The transfer function of these filters is represented as follows:

$$LPF(s) = \frac{\omega_{cut}^2}{s^2 + 2\zeta\omega_{cut}s + \omega_{cut}^2} \qquad (10)$$

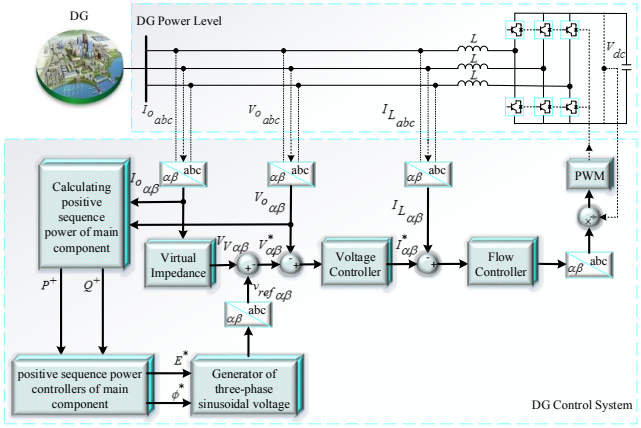

Fig. 2. The proposed control method

Transmission to frame $\alpha\beta$ was determined according to the following equation:

$$x_{\alpha\beta} = \begin{bmatrix} \cos(\theta) & -\sin(\theta) \\ \sin(\theta) & \cos(\theta) \end{bmatrix} . x_{dq} \qquad (11)$$

The details of the transformation is shown in *dq*/$\alpha\beta$ transformation block in Fig. 2. The control was calculated using the characteristics shown by the equations (3) and (4). Since a balanced electrical system was considered in this

section, the total power of the main component can be related to positive sequence, which was the reason for not using the *"+"* superscript for P and Q. In the following sections, details of the other blocks of DG control system will be described.

III. Simulation and Results

The tests and validation processes are categorized into three main parts, as shown Fig. 3.

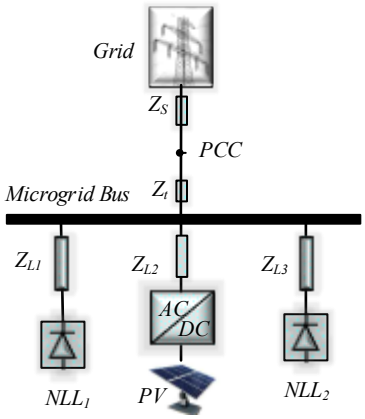

Fig. 3. System configuration with PV and nonlinear loads

The performance of the PV and nonlinear loads in microgrid without compensation devices is described in the first part of this section. The second part of this section verifies the performance of the suggested proposed controller under unbalanced, and nonlinear load situations. The system is assumed to be radial with several feeders and a collection of nonlinear loads.

This MG includes the PV which is connected to the grid by the power electronic interface devises. The proposed control methods are applied to the PV. Another side of this system consists of two nonlinear loads (NLL), such as the three unbalanced single-phase diode rectifiers and the three-phase diode rectifier, which produced the distorted and unbalanced waveform.

The grid connected inverters and NLLs make the system current nonlinear and unbalanced and also require the injection of harmonic currents into the microgrid.

The parameters of the three-phase power line, nonlinear load and PV parameters can be found in Table 1 and Table 2, respectively.

TABLE I. Power Line Parameters

Parameters	ZL1	ZL2	ZL3
R (Ω)	0.54	0.16	0.29
L (mH)	1.4	0.38	0.67

TABLE II. PV and Nonlinear Loads Parameters

Load/RERs	Parameters	Values
Photovoltaic	Inverter switching frequency	4 kHz
	Inverter resistance	0.2 mΩ
	Inverter capacitance	5 µF
	DC-link voltage	745 V
Three unbalanced single-phase diode rectifiers (NLL1)	RL	30 kW, 10 kVAr
Three-phase diode rectifier (NNL2)	Resistor	0.3 Ω

The uncompensated nonlinear load 1 (NLL1) current waveforms is shown in Fig 4. This figure shows the currents NLL1, equipped without any compensation devices and connected to microgrid. The current is 26.97 (A) and the THD is 5.88%.

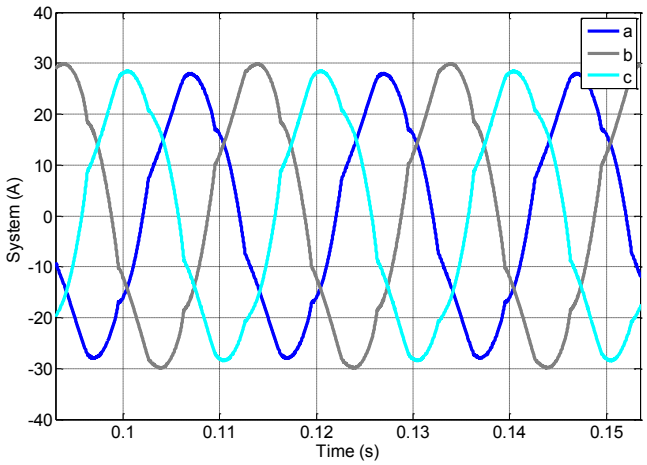

Fig. 4. Unbalanced current waveforms of NLL1

Fig. 5 presents the waveforms of the currents under the condition of nonlinear load 2 and without compensation devices. The current is 117.9 (A) and the THD is 17.51%.

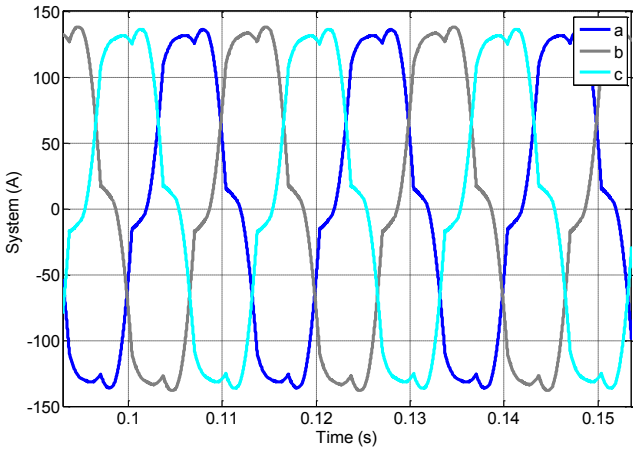

Fig. 5. Distortion current waveforms of NLL2

Fig. 6 shows the distorted current waveforms of PV and nonlinear loads. In this case, PV and nonlinear loads are connected to the grid as microgrid.

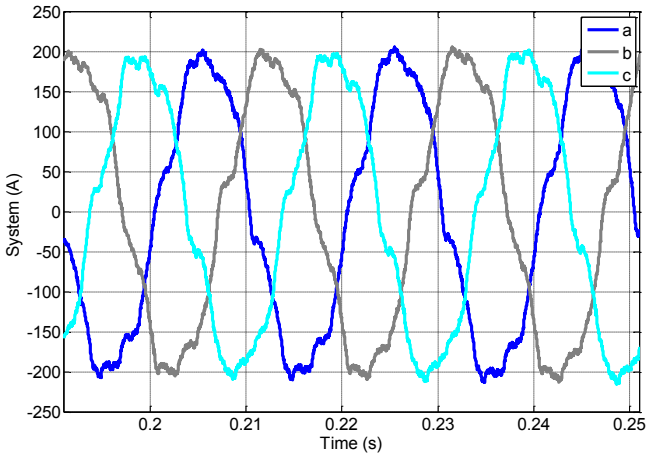

Fig. 6. System distortion current waveforms under the condition of all loads/PV in operation

The proposed control method is effective in correcting the distortion. Fig. 7 shows the effective compensation values of the harmonic current for the PV.

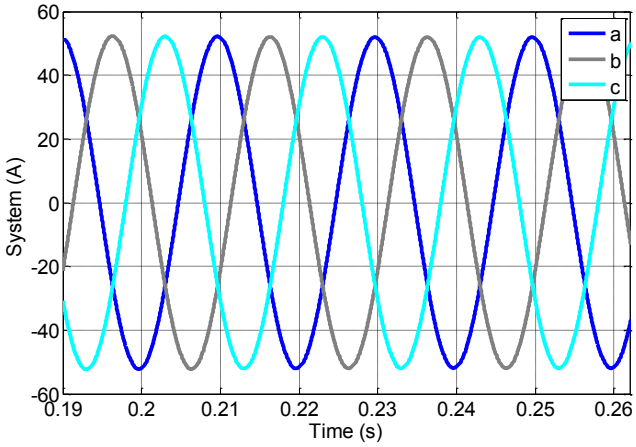

Fig. 7. Current waveforms of the System

Fig. 7 shows the current waveforms of PV and nonlinear load 1 and 2 together. In this case, the THD in the system is 2.47%. Thus, this approach is verified to be capable of meeting IEEE 519-1992 recommended harmonic standard limits.

IV. Conclusion

This paper proposed a method to minimize the current harmonic contents collectively in a three-phase photovoltaic grid connected inverters, subjected to nonlinear and unbalanced load conditions. The proposed control method is effective in correcting the distortion. The results show the effectiveness of proposed control method in reducing the THD to less than 3% while simultaneously stabilizing any imbalance in the system.

Acknowledgment

The authors wish to thank the Ministry of Education (MOE) and Universiti Teknologi Malaysia under the Post-Doctoral Fellowship Scheme grant numbers, 4F828, 04E54, and 18H10 for the financial support.

References

[1] A. Khaledian, B. Vahidi, and M. Abedi, “Harmonic Distorted Load Control in a Microgrid,” J. Appl. Res. Technol., vol. 12, no. 4, pp. 792–802, 2014.

[2] A. Naderipour, A. Asuhaimi Mohd Zin, M. H. Bin Habibuddin, M. R. Miveh, and J. M. Guerrero, “An improved synchronous reference frame current control strategy for a photovoltaic grid-connected inverter under unbalanced and nonlinear load conditions,” PLoS One, vol. 12, no. 2, pp. 1–17, 2017.

[3] A. Naderipour, Z. Abdul-Malek, M. Miveh, M. Hadidian Moghaddam, A. Kalam, and F. Gandoman, “A Harmonic Compensation Strategy in a Grid-Connected Photovoltaic System Using Zero-Sequence Control,” Energies, vol. 11, no. 10, p. 2629, 2018.

[4] A. Mohd Zin, A. Naderipour, M. Hafiz Habibuddin, and J. Guerrero, “Harmonic currents compensator GCI at the microgrid.”

[5] Z. Zeng, H. Yang, R. Zhao, and C. Song, “A novel control strategy for grid-connected inverters with LC filter based on passive Hamiltonian theory,” Dianwang Jishu/Power Syst. Technol., vol. 36, no. 4, pp. 37–42, 2012.

[6] D. Dong, B. Wen, D. Boroyevich, P. Mattavelli, and Y. Xue, “Analysis of phase-locked loop low-frequency stability in three-phase grid-connected power converters considering impedance interactions,” IEEE Trans. Ind. Electron., vol. 62, no. 1, pp. 310–321, 2015.

[7] N. Jelani and M. Molinas, “Shunt active filtering by constant power load in microgrid based on IRP pq and CPC reference signal generation schemes,” in Power System Technology (POWERCON), 2012 IEEE International Conference on, 2012, pp. 1–6.

[8] C. T. V. Chunkag and P. Thounthong, “Control of single-phase AC to DC converter for hybrid microgrid,” in Proceedings of the International Conference on Power Electronics and Drive Systems, 2013, pp. 668–673.

[9] S. Sahoo, S. Prakash, and S. Mishra, “Investigation of voltage template based control of a grid connected DC microgrid under different grid conditions,” in 2016 IEEE 6th International Conference on Power Systems, ICPS 2016, 2016, pp. 1–6.

[10] W. Al-Saedi, S. W. Lachowicz, D. Habibi, and O. Bass, “Voltage and frequency regulation based DG unit in an autonomous microgrid operation using Particle Swarm Optimization,” Int. J. Electr. Power Energy Syst., vol. 53, no. 1, pp. 742–751, 2013.

[11] S. Fukuda and T. Yoda, “A novel current-tracking method for active filters based on a sinusoidal internal model,” IEEE Trans. Ind. Appl., vol. 37, no. 3, pp. 888–895, 2001.

[12] R. Teodorescu, F. Blaabjerg, and M. Liserre, “Proportional-resonant controllers. A new breed of controllers suitable for grid-connected voltage-source converters,” in OPTIM 2004, Brasov, Romania, 2004.

IEEE